

Optical and magnetic properties of $\text{Co}_3\text{O}_4/\text{ZnO}$ Core/Shell nanoparticles

A. ESMAIELZADEH KANDJANI*, S. E. HASHEMI AMIRI, M. R. VAEZI, S. K. SADRNEZHAAD
Materials and Energy Research Center (MERC), Karaj, Iran

$\text{Co}_3\text{O}_4/\text{ZnO}$ core/shell nanoparticles have been synthesized via hydrothermal/sol-gel routes. The obtained core and core/shell nanoparticles were investigated for their structures, morphologies, specific surface area, optical absorption and magnetic properties using x-ray diffraction (XRD), transition electron microscopy (TEM), Brunauer-Emmett-Teller (BET), ultraviolet-visible spectroscopy (UV-Vis) and vibrating sample magnetometer (VSM), respectively. From TEM images, it can be shown that ZnO shell has been properly formed on Co_3O_4 cores. Due to applying thick ZnO shells on Co_3O_4 cores, Co_3O_4 peaks were faded or just tiny peaks of them existed in core/shell XRD patterns. Also, from TEM images, the mean nanoparticle sizes for core and core/shell were estimated to be 22 and 56nm, respectively. The existence of ZnO shells on the Co_3O_4 nanoparticles affects the final band gap and shows a blue shift in band gap of ZnO. Also, the obtained results show that existence of Co_3O_4 in core of ZnO changes diamagnetic ZnO shell into weak ferromagnetic material.

(Received July 26, 2010; accepted October 14, 2010)

Keywords: Core/Shell nanoparticles, Cobalt oxide, Zinc oxide, Soft chemical synthesis

1. Introduction

By emerging nano-materials a tremendous effort has been carrying out for investigating on their significant properties which make progressive improvements in many scientific fields. Among these nano-materials, nano-semiconductor materials have become one of the major fields in which attentions of different researchers, from bioscience to optoelectronics, have been attracted due to unique properties of these nanoparticles and dependency of their final properties on the size of particles. Nano-photocatalysts are one of the well known subroutine categories of semiconductors' applications. Their advanced and vast applications including cancer treatment [1], purification and sterilization of water and air [2], self cleaning coatings [3], etc make them one of the most important nano materials for daily uses.

Cancer is the top cause of the death in the world wide. Conventional methods for cancer treatments, surgical, radiological, immunological, thermo-therapeutic, and chemo-therapeutic treatments are well-known. The first attempts for cancer treatment by photocatalysts are related to A. Fujishima et al. efforts, in which TiO_2 nanoparticles were injected in the cancer tumors and exposed to high intensities of light. The results indicated on the fact that nano-photocatalysts can inhibit the tumor growth [4]. Also, high ratio of surface to volume in nanoparticles causes the surface reactions occur better by contributing of major numbers of consisting molecules of a particle in surface reactions [5]. Regardless the considerable benefits of nano-drugs, the side effects of nano material usage are considerable. The inability in controlling drug delivery endangers healthy cells on chemical toxicity. Thus, nowadays production of well controllable delivery systems has been increasing among researchers.

In environmental applications, un-purified water which contains considerable amounts of photocatalysts could become a problem. By exposing light to the remained photocatalysts, for each photon an electron-hole pair produces and subsequently it degrades the adjacent media [5]. Due to unselective manner of aforementioned phenomenon, harmful and useful cells both are attracted with produced electron-hole pairs. The conventional methods for separating nano-particles from the media have low efficiency as well as high costs [6]. Also, two major properties should be considered while using photocatalysts: specific surface area and band gap energy of prepared photocatalysts. High amount of specific surface area is one of the main functional variables for adsorbing cells on particles surface and increasing the active sites for photocatalytic reactions [6]. On the other hand, most of the photocatalytic properties of semiconductors are related to their optical band gap. These properties show the workability of a photocatalyst.

Core/shell nanocomposites are one of the solutions for many difficulties in which a bifunctional nano-architecture or a modification in properties, which can't be achieved by using one type of nano-particles, is needed [7,8]. Using a magnetic core enables directing particle using safe external magnetic field [9]. If a core/shell composite contains magnetic core and semiconductor shell with high surface area and proper photocatalytic properties, the delivery and also purification of the particles become possible.

Co_3O_4 is a well known magnetic p-type semiconductor material. The performance of tri-cobalt tetra-oxide particles is highly dependent on the nanoparticles size and their specific surface areas [10].

Thus, many attempts have been done to synthesize Co_3O_4 with high specific surface area and low dimension, such as sol-gel [11], thermal decomposition of solid phase [12], chemical vapor deposition (CVD) [13] and hydrothermal methods [14]. Among these, hydrothermal processing is widely used due to production of fine and uniform structures with high controllability in growth and also it can be used for preparation of fine and uniform nano- Co_3O_4 particles.

Zinc oxide (ZnO) is one of the most important semiconductors. This material in nano scale shows specific properties which make it applicable as promising photocatalysts, light emitting diode, sterilization, etc [15-17]. Many different chemical approaches have been reported for synthesizing ZnO nanoparticles such as hydrothermal, sonochemical, sol-gel, etc [18-21]. Among these synthetic routes, sol-gel is known as one of the main synthesis routes for applying homogenous films on different surfaces and particles and thus, it is one of the main and important routes for making core/shell heterostructures.

In the present work, we report a promising route for synthesizing $\text{Co}_3\text{O}_4/\text{ZnO}$ core/shell via soft chemical route. H_2O_2 -assisted hydrothermal method was used for synthesizing Co_3O_4 core nanoparticles, while ZnO shell was obtained via sol-gel method. Structure, morphology, specific surface area and magnetization were investigated for obtained particles using XRD, SEM, BET and VSM analysis, respectively. UV-Vis was used for investigating linear optical properties of obtained nanoparticles.

2. Experimental

2.1 Materials

NH_4OH , H_2O_2 , $\text{Co}(\text{Ac})_2$, $\text{Zn}(\text{Ac})_2$, triethanolamin (TEA) (purchased from Merck) were used as starting materials. They were in analytical grade and were used without further purification.

2.2. Synthesis

2.2.1. Core nanoparticles

NH_4OH aqueous solution (50ml, pH=10) with 25ml of H_2O_2 were added drop by drop to $\text{Co}(\text{Ac})_2$ aqueous solution (0.1 M, 50ml) in 30 minutes. The obtained solution was poured into 90ml Teflon lined autoclaves and filled up to 80% of its volume. Then, the autoclaves were kept at 180°C for 24 hours. After that, the autoclaves were cooled to room temperature naturally, and precipitates were filtered and washed with distilled water and ethanol for several times. Finally, the obtained powders were dried at 50°C for 24 hours. The procedures are shown in Fig. 1.

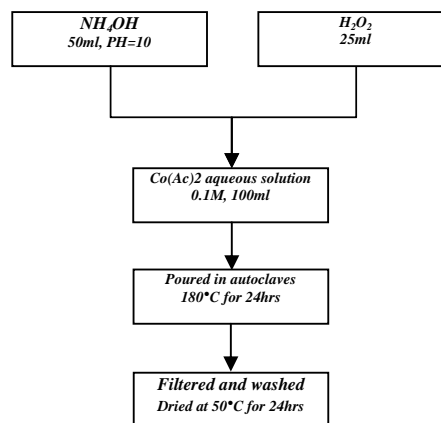


Fig. 1. Flowchart for synthesizing Co_3O_4 nanoparticles.

2.2.2. Core/shell nanoparticles

A simple sol-gel procedure was used for producing ZnO shells on the Co_3O_4 nanoparticles. 0.3 g Co_3O_4 was dispersed in 50 ml solution of pure methanol and TEA with weight ratio of $\left[\frac{\text{TEA}}{\text{Zn}(\text{Ac})_2} = 1\right]$. Another solution prepared by dissolving $\text{Zn}(\text{Ac})_2$ in 50 ml deionised water. The concentration of $\text{Zn}(\text{Ac})_2$ in final solution was 0.3 M. Both solutions were sonicated for 30 min. then, the second solution poured into the first solution under stirring condition and was kept for 2 hours at 60°C . The obtained core/shell particles were filtered and dried at 50°C for 24 hours. Then, the dried powder was calcinated for 2 hours at 450°C . The schematic diagram of procedure is shown in Fig. 2.

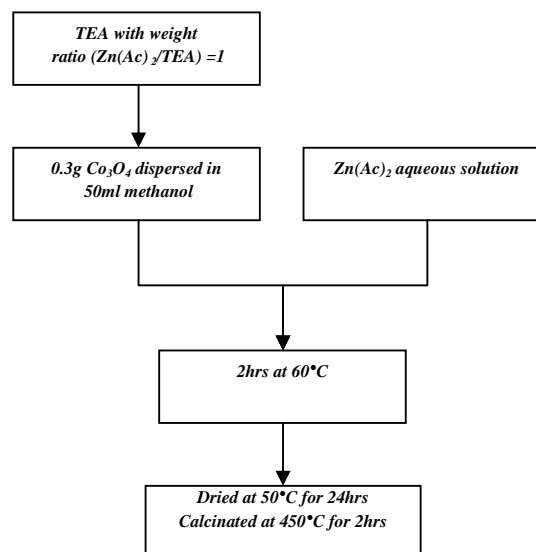


Fig. 2. Flowchart for synthesizing $\text{Co}_3\text{O}_4/\text{ZnO}$ nanoparticles.

2.3. Analyses

The crystalline structure of materials was studied using Siemens D-5000 X-ray diffractometer (XRD) with Cu-K_α radiation ($\lambda=0.154178\text{nm}$). Scanning Electron Microscopy (Philips XL30) images were used for studying morphologies of prepared samples. The optical properties were studied by double-beam Shimadzu UV-2450 Scan UV-Visible.

3. Results and discussion

XRD patterns of synthesized nanoparticles are shown in Fig. 3. As it can be seen from Fig. 3, the peaks are attributed to Co₃O₄ (JCPDF 42-1467) for core nanoparticles and no other peak is detected while in core/shell just some undetectable traces can be detected from core nanoparticles. In core/shell nanoparticles, all major peaks are contributed to wurtzite ZnO (JCPDF 36-1451). The main reason for fading core particles in the XRD pattern of core/shell can be related to considerable amounts of ZnO nanoparticles synthesized adjacent to core nanoparticles.

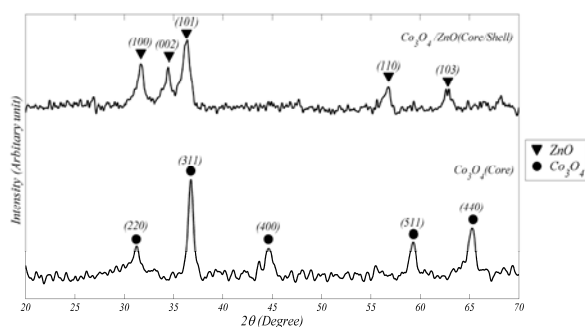


Fig. 3. XRD patterns of core and core/shell nanoparticles.

If thickness of produced shell films on the surface of the core particles were considerable in comparison with core nanoparticles, a reduction in the intensity of core peaks can be detected. Also, if the mass fraction of produced shell was much more than used core nanoparticles, it could result in reduction of core peaks in XRD patterns. The mentioned phenomena can intensify reduction in peaks intensities of core nanoparticles and also increase the noises in the core/shell patterns [22].

TEM images for the obtained core and core/shell nanoparticles are shown in Fig. 4. It can be seen that the median particle size of Co₃O₄ is about 22nm where in core/shell nanoparticles, existence of the shell around the core particles makes the particles bigger and thus the median particle size is about 56nm. Also, the darker parts of the image (Fig. 4b) in core/shell are related to core where brighter ones are related to ZnO shells. From BET analysis, the specific surface areas for core and core/shell were detected 98.6 and 54.6m²/g, respectively. BET adsorption isotherms for core and core/shell are shown in

Fig. 5. The plotted isotherms represent highly isotherm of Type III. It has been shown, if a solid contains no porosity, its isotherm tends to appear as a Type III isotherm [23]. Also, decrease in the specific surface area could be another reason for formation and growth of ZnO shells on Co₃O₄ surface and subsequent decrease in specific surface area.

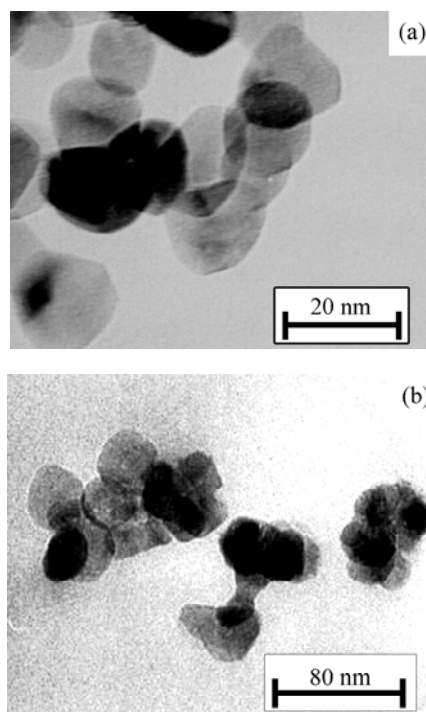


Fig. 4. TEM images of a) core and b) core/shell nanoparticles.

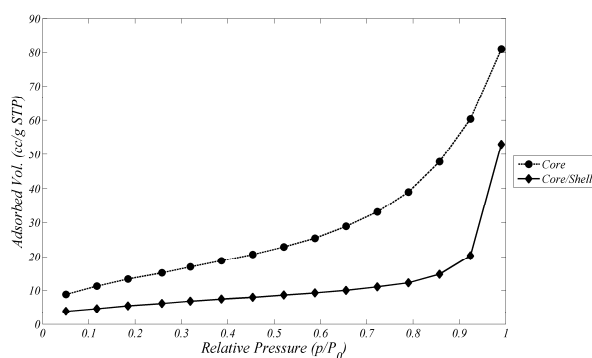


Fig. 5. BET adsorption isotherms.

Optical absorptions of the obtained nanoparticles are shown in Fig. 6. Absorption coefficient, $\alpha(\lambda)$, for allowed direct transition of semiconductors is given by the following expression [24]:

$$\alpha = A \frac{(h\nu - E_g)^{0.5}}{h\nu} \quad (1)$$

where A is coefficient of the given electronic transition probability, E_g is band gap energy and n is equal to 0.5 and 2 for allowed direct and indirect transitions and 1.5 and 3 in case of forbidden direct and indirect transitions, respectively. In current study, the best fit of $(\alpha h\nu)^{1/n}$ versus photon energy was obtained 0.5 for both of core and core/shell.

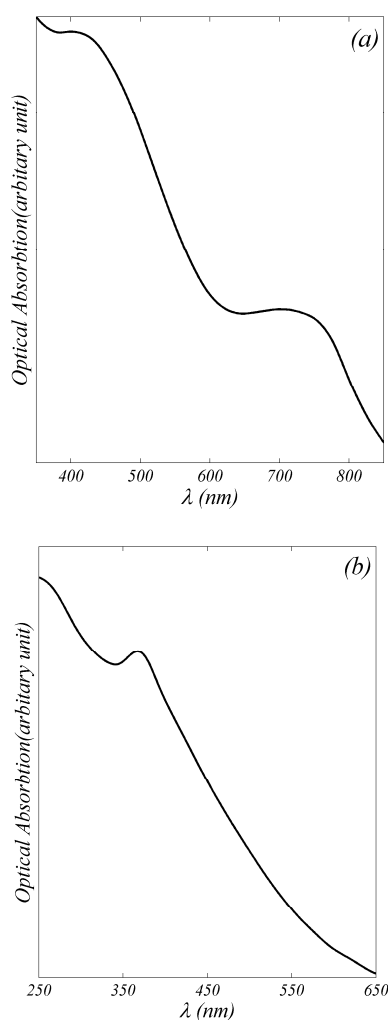


Fig. 6. UV-Vis spectra of a) core and b) core/shell nanoparticles.

Fig. 7 shows plots of $(\alpha h\nu)^{1/n}$ versus photon energy for both core and core/shell nanoparticles. As can be seen from these plots, in core (Fig. 7a) there are two regions in optical absorption. First one with 1.89 eV energy is related to nature of spinel structure of Co_3O_4 . In spinel structure of Co_3O_4 , Co(III) ions locate in center of structure. This fact affects the band structure and thus, gives rise to a subband in the bandgap energies. Thus two bands could be detected in absorptions, first related to excitation of $\text{O}(\text{II}) \rightarrow \text{Co}(\text{III})$ which results in emerging 2nd band gap energy in 1.4 eV [25,26]. This gap should be located inside of band gap and thus the bandgap should have larger

amounts. 1.89 eV is the real optical band gap of Co_3O_4 . The band gap shows a reduction in comparison with bulk Co_3O_4 , there are many reports in which main reason for red shift in nano Co_3O_4 was contributed to quantum-confinement effects [27].

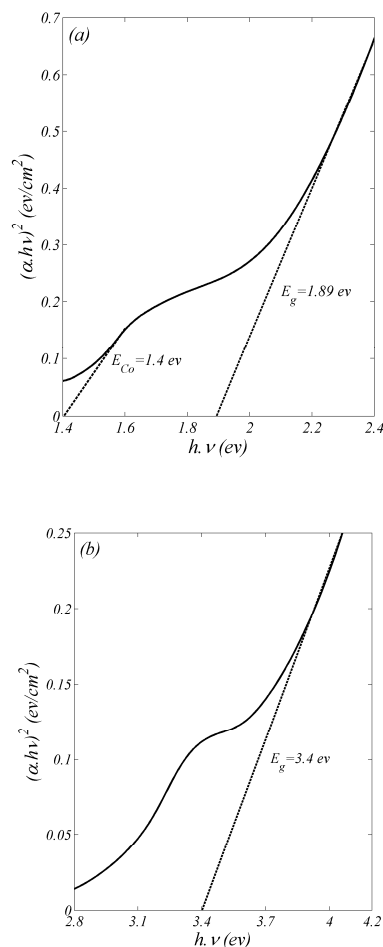


Fig. 7. $(\alpha h\nu)^{1/n}$ vs. photon energy for obtained a) Co_3O_4 and b) $\text{Co}_3\text{O}_4/\text{ZnO}$.

The optical properties of Core/shell are somehow different from core itself (Fig. 7b). As could be seen in Fig. 6, the obtained band gap is 3.42 eV which shows a blue shift in comparison with bulk ZnO ($E_g=3.3\text{eV}$). In our previous work, we reported red shift in ZnO band gap ($E_g=3.27\text{eV}$) prepared by same way [20]. This blue shift could be resulted from two phenomena: first, in large band gap semiconductors, mainly, a reduction in size results in an extension in band gaps [28]. As shown in TEM images some parts of ZnO shells in nanocomposite are thinner than 25 nm, which could make a blue shift. Also, The existence of exciton shoulder in absorption spectra of nanocomposite is another claim for making ZnO with thicknesses low enough for emerging exciton shoulder at room temperature which has been seen in other nano-semiconductors too [29]. Second, existence of p-type

Co₃O₄ in core adjacent to n-type ZnO affects the final properties of nanocomposite and makes a blue shift in final optical band gap of nanocomposite.

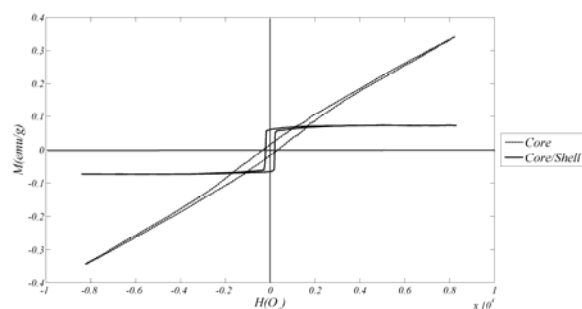


Fig. 8. VSM spectra of a) core and b) core/shell nanoparticles.

Fig. 8 shows magnetic behaviours of Co₃O₄ and Co₃O₄/ZnO core/shells also in Table 1 the magnetic properties of prepared materials are listed. Co₃O₄ due to its spinel structure shows anti-ferromagnetic characteristics [30], however, the core shows dilute ferromagnetic characteristic. This might be due to existence of oxygen in spinel structure of Co₃O₄ which avoids direct interaction of magnetic momentums [31].

As could be seen from this table, the amount of saturation magnetism in core/shell nanocomposites shows a decrease in comparison with core. In core/shell Co₃O₄/ZnO nanocomposites there are two phenomena. ZnO is a diamagnetic material. These materials in VSM analysis show a negative magnetization and no hysteresis loop. ZnO can change its magnetic characteristic by doping of some impurities such as Co, Mn, Ni, etc. These dilute dopants can change the diamagnetic behaviour of ZnO into carrier induced ferromagnetic materials [32]. Existence of Co₃O₄ core adjacent to ZnO films results in a dilute ferromagnetic characteristic due to ability in ordering disorder spins arrays in surface of Co₃O₄ which in magnetic field could be ordered and compensation diamagnetic characteristic of shell component. On the other hand, by applying a diamagnetic shell on a magnetic material, saturation magnetism of core decreases. This decrease could be intensified by thickening of diamagnetic shell.

4. Conclusions

Co₃O₄/ZnO core/shell particles were synthesized properly through soft chemical methods. The main characteristics of prepared nanocomposites can be explained as:

1. Synthesizing small core nanoparticles via one step hydrothermal synthesis route with mean particle size of 22 nm.
2. Proper applying ZnO thin films on core nanoparticles using a simple sol-gel route with mean particle size of 56 nm.

3. Ability in modifying band gap of active surface semiconductor (ZnO) by using Co₃O₄ in core and proper controlling of shell thickness.

4. Ability to control final core/shell with proper magnetic sources due to modifying diamagnetic ZnO into weak ferroelectric material by using Co₃O₄ nanoparticles as core.

The findings show that using Co₃O₄ as a core for ZnO it can be produced a weak ferromagnetic photocatalyst which could be a solution for side effects of using diamagnetic photocatalysts in many applications.

Reference

- [1] R. Cai, K. Hashimoto, K. Itoh, Y. Kubota, A. Fujishima, *Bull. Chem. Soc. Jpn.* **64**, 1268 (1991).
- [2] N. Daneshvar, M.H. Rasoulifard, A.R. Khataee, F. Hosseinzadeh, *J. Hazard. Mater.* **143**, 95 (2007).
- [3] R. Wang, K. Hashimoto, A. Fujishima, M. Chikuni, E. Kojima, A. Kitamura, M. Shimohigoshi, T. Watanabe, *Adv. Mater.*, **10**, 135 (1998).
- [4] A. Fujishima, J. Ohtsuki, T. Yamashita, S. Hayakawa, *Photomed. Photobiol.* **8**, 45 (1986).
- [5] V. Ramamurthy, K.S. Schanze (eds), *Molecular and supramolecular photochemistry*, New York, Marcel Dekker Inc., 2003.
- [6] T. Oppenlander, *Photochemical Purification of Water and Air*, Weinheim, Wiley-VCH, 2003.
- [7] A.V. Goncharenko, *Chem. Phys. Lett.* **386**, 25 (2004).
- [8] A.V. Goncharenko, Y. Ch. Chang, *Chem. Phys. Lett.* **439**, 121 (2007).
- [9] W. Zhao, J. Gu, L. Zhang, H. Chen, J. Shi, *J. Am. Chem. Soc.*, **127**, 8916 (2005).
- [10] R. V. Narayan, V. Kanniah, A. Dhathathreyan, *J. Chem. Sci.*, **118**, 179 (2006).
- [11] M. E. Baydi, G. Poillerat, J. L. Rehspringer, J. L. Gautier, J.F. Koenig, P. Chartier, *J. Solid State Chem.*, **109**, 281 (1994).
- [12] Y. Hua-Ming, H. Yue-Hua, Z. Xiang-Chao, Q. Guan-Zhou, *Mater Lett.* **58**, 387 (2004).
- [13] C. S. Cheng, M. Serizawa, H. Sakata, T. Hirayama, *Mater. Chem. Phys.* **53**, 255 (1998).
- [14] W. Zhao, Y. Liu, H. Li, X. Zhang, *Mater Lett.* **62**, 772 (2008).
- [15] R. Y. Hong, J. H. Li, L. L. Chen, D. Q. Liu, H. Z. Li, Y. Zheng, J. Ding, *Powder Technol.* **189**, 426 (2009).
- [16] X. M. Zhang, M. Y. Lu, Y. Zhang, L. J. Chen, Z. L. Wang, *Adv. Mater.* **21**, 2767 (2009).
- [17] U. Ozgur, Y. I. Alivov, C. Liu, A. Teke, M. A. Reshchikov, S. Dogan, V. Avrutin, S. J. Cho, H. Morkoc, *J. Appl. Phys.*, **98**, 041301 (2005).
- [18] B. Baruwati, D. Kishore-Kumar, S. V. Manorama, *Actuat. B-Chem.*, **119**, 676 (2006).
- [19] A. Esmailzadeh Kandjani, M. Farzalipour Tabriz, B. Pourabbas, *Mater. Res. Bull.* **43**, 645 (2008).
- [20] A. Esmailzadeh Kandjani, A. Shokuhfar, M. Farzalipour Tabriz, N. A. Arefian, M. R. Vaezi

- J. Optoelectron. Adv. Mater. **11**, 289 (2009).
- [21] A. Esmailzadeh Kandjani, M. Farzalipour Tabriz, N. A. Arefian, M. R. Vaezi, S. Ahmadi Kandjani, J. Optoelectron. Adv. Mater. **12**, 1421 (2010).
- [22] J. N. Gillet, M. Meunier, J. Phys. Chem. B **109**, 8733 (2005).
- [23] S. J. Gregg, K. S. W. Sing, Adsorption, Surface area and Porosity, (2nd ed.), London, Academic Press, 1982.
- [24] J. J. Ramsden, M. Gratzel, J. Chem. Soc., Faraday Trans. **80**, 919 (1984).
- [25] I. D. Belova, Y. E. Roginskaya, R. R. Shifrina, S. G. Gagarin, Y. V. Plekhanov, Y. N. Venevtsev, Solid State Commun. **47**, 577 (1983).
- [26] J. G. Cook, M. P. Van Der Meer, Thin Solid Films, **144**, 165 (1986).
- [27] Y. Zhang, Y. Chen, T. Wang, J. Zhou, Y. Zhao, Micropo. Mesopor. Mat., **114**, 257 (2008).
- [28] M. Li, J.C. Li, Mater. Lett., **60**, 2526 (2006).
- [29] J. Nanda, S. Sapra, D.D. Sarma, Chem. Mater. **12**, 1018 (2000).
- [30] H.T. Zhua, J. Luo, J. K. Liang, G. H. Rao, J.B. Li, J. Y. Zhang, Z.M. Du, Physica B, **403**, 3141 (2008).
- [31] D. Vollath, Nanomaterials, Germany, Wiley-VCH, 2008.
- [32] H. Morkoc, U. Mitozgur, Zinc Oxide, Fundamentals, Materials and Device Technology, Germany, WILEY-VCH, 2009.

*Corresponding author: MSTGAhmad@Gmail.com